

# Baryon chiral perturbation theory transferred to hole-doped antiferromagnets on the honeycomb lattice

**F-J Jiang<sup>1</sup>, F Kämpfer<sup>2</sup>, B Bessire<sup>3</sup>, M Wirz<sup>4</sup>, C P Hofmann<sup>5</sup>, and U-J Wiese<sup>6</sup>**

<sup>1</sup> Department of Physics, National Taiwan Normal University, 88, Sec. 4, Ting-Chou Rd. Taipei 116, Taiwan

<sup>2</sup> BKW FMB Energy Ltd, Energy Trading Unit, 3000 Bern, Switzerland

<sup>3</sup> Institute of Applied Physics, Bern University, Sidlerstrasse 5, CH-3012 Bern, Switzerland

<sup>4</sup> Mathematical Institute, Bern University, Sidlerstrasse 5, CH-3012 Bern, Switzerland

<sup>5</sup> Facultad de Ciencias, Universidad de Colima, Bernal Díaz del Castillo 340, Colima C.P. 28045, Mexico

<sup>6</sup> Institute for Theoretical Physics, Albert Einstein Center for Fundamental Physics, Bern University, Sidlerstrasse 5, CH-3012 Bern, Switzerland

E-mail: christoph.peter.hofmann@gmail.com

**Abstract.** A systematic low-energy effective field theory for hole-doped antiferromagnets on the honeycomb lattice is constructed. The formalism is then used to investigate spiral phases in the staggered magnetization as well as the formation of two-hole bound states.

## 1. Motivation

Although the phenomenon of high-temperature superconductivity was discovered more than twenty-five years ago [1], the dynamical mechanism behind it still remains a mystery today. The reason may be readily identified: Due to the nonperturbative nature of the problem, analytic studies usually suffer from uncontrolled approximations, while numerical simulations of the microscopic Hubbard and  $t$ - $J$ -type models suffer from a severe fermion sign problem away from half-filling.

In the present work, we will address the physics of the antiferromagnetic precursors of high-temperature superconductivity from a universal and model-independent point of view, based on the method of effective Lagrangians. The effective Lagrangian method is very well-established in particle physics, where chiral perturbation theory (CHPT) [2, 3] represents the effective theory of quantum chromodynamics (QCD). It operates in the Goldstone boson sector of QCD, taking into account the octet of the pseudoscalar mesons that emerge due to the spontaneously broken chiral symmetry. Baryon chiral perturbation theory [4, 5, 6, 7] is an extension of CHPT as it also includes heavy particles such as the baryon octet or decuplet, i.e. those degrees of freedom that remain massive in the chiral limit.

Spontaneous symmetry breaking is also a very common phenomenon in condensed matter physics: Magnons e.g. are the Goldstone bosons of a spontaneously broken spin symmetry  $SU(2)_s \rightarrow U(1)_s$ , while phonons emerge due to a spontaneously broken translation symmetry.

For these systems effective Lagrangians have been constructed in Refs. [8, 9, 10, 11] and various applications have been considered in Refs. [12, 13, 14, 15, 16, 17, 18].

However, the incorporation of heavy degrees of freedom in the condensed matter domain – in a transparent and systematic manner – has only been achieved recently. An effective theory for weakly doped antiferromagnets, the analog of baryon chiral perturbation theory, has been constructed for hole- and electron-doped antiferromagnets on the square lattice in Refs.[19, 20, 21] and for hole-doped antiferromagnets on the honeycomb lattice in Ref.[22]. Further applications of the formalism were discussed in Refs.[23, 24, 25], demonstrating that the effective Lagrangian method allows one to gain insight into the physics of these insulating precursors of high-temperature superconductors in a systematic and unambiguous manner.

In this presentation we will focus on hole-doped antiferromagnets on a honeycomb lattice. We first review the systematic construction of the effective Lagrangian for magnons and holes for these systems and will then consider two applications of the formalism: The emergence of spiral phases in the staggered magnetization order parameter as well as the formation of two-hole bound states mediated by magnon exchange.

We would also like to point out that in a recent article on an analytically solvable microscopic model for a hole-doped ferromagnet in 1+1 dimensions [26], the correctness of the effective field theory approach was demonstrated by comparing the effective theory predictions with the microscopic calculation. Likewise, in a series of high-accuracy investigations of the antiferromagnetic spin- $\frac{1}{2}$  quantum Heisenberg model on a square lattice using the loop-cluster algorithm [27, 28, 29, 30], the Monte Carlo data were confronted with the analytic predictions of magnon chiral perturbation theory and the low-energy constants were extracted with permille accuracy. All these tests unambiguously demonstrate that the effective Lagrangian approach provides a rigorous and systematic derivative expansion for both ferromagnetic and antiferromagnetic systems.

## 2. Construction of the effective field theory for holes and magnons

The effective Lagrangian approach is based on a symmetry analysis of the underlying theory, i.e., in the present case the Hubbard or  $t$ - $J$ -type models which are believed to be minimal models for high-temperature superconductors [31]. We thus first perform a rigorous symmetry analysis of these models in order to then construct the effective Lagrangian for holes and magnons.

### 2.1. Symmetry analysis

Let  $c_{xs}^\dagger$  denote the operator which creates a fermion with spin  $s \in \{\uparrow, \downarrow\}$  on a lattice site  $x = (x_1, x_2)$ . The corresponding annihilation operator is  $c_{xs}$ . These fermion operators obey the canonical anticommutation relations

$$\{c_{xs}^\dagger, c_{ys'}\} = \delta_{xy}\delta_{ss'}, \quad \{c_{xs}, c_{ys'}\} = \{c_{xs}^\dagger, c_{ys'}^\dagger\} = 0. \quad (1)$$

The second quantized Hubbard Hamiltonian is defined by

$$H = -t \sum_{\langle x,y \rangle; s=\uparrow, \downarrow} (c_{xs}^\dagger c_{ys} + c_{ys}^\dagger c_{xs}) + U \sum_x c_{x\uparrow}^\dagger c_{x\uparrow} c_{x\downarrow}^\dagger c_{x\downarrow} - \mu' \sum_{x; s=\uparrow, \downarrow} c_{xs}^\dagger c_{xs}, \quad (2)$$

where  $\langle x, y \rangle$  indicates summation over nearest neighbors,  $t$  is the hopping parameter, and the parameter  $U > 0$  fixes the strength of the Coulomb repulsion between two fermions located on the same lattice site. The parameter  $\mu'$  denotes the chemical potential.

Using the fermion creation and annihilation operators, we define the following  $SU(2)_s$  Pauli spinors

$$c_x^\dagger = \begin{pmatrix} c_{x\uparrow}^\dagger & c_{x\downarrow}^\dagger \end{pmatrix}, \quad c_x = \begin{pmatrix} c_{x\uparrow} \\ c_{x\downarrow} \end{pmatrix}. \quad (3)$$

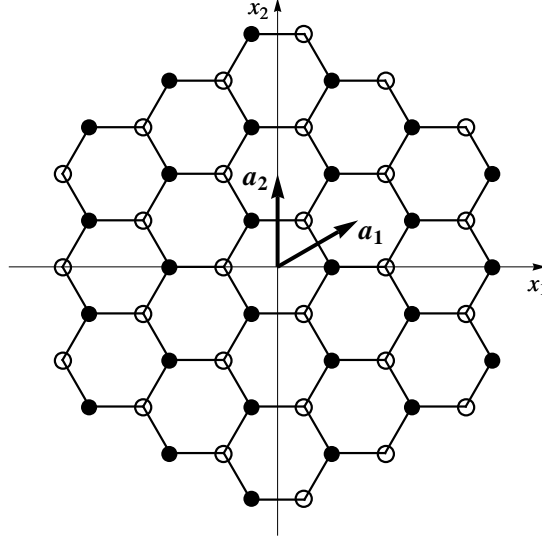


**Figure 1.** Bipartite non-Bravais honeycomb lattice consisting of two triangular Bravais sublattices. The translation vectors are  $a_1$  and  $a_2$ .

In terms of these operators, the Hubbard model can be reformulated as

$$H = -t \sum_{\langle xy \rangle} (c_x^\dagger c_y + c_y^\dagger c_x) + \frac{U}{2} \sum_x (c_x^\dagger c_x - 1)^2 - \mu \sum_x (c_x^\dagger c_x - 1). \quad (4)$$

The parameter  $\mu = \mu' - \frac{U}{2}$  controls doping where the fermions are counted with respect to half-filling.

Since all terms in the effective Lagrangian must be invariant under all symmetries of the Hubbard model, a careful symmetry analysis of Eq.(4) is needed. Let us divide the symmetries of the Hubbard model into two categories: Continuous symmetries, which are internal symmetries of Eq.(4), and discrete symmetries, which are symmetry transformations of the underlying honeycomb lattice depicted in figure 1.

The continuous symmetries are the  $SU(2)_s$  spin rotation symmetry, the  $U(1)_Q$  fermion number symmetry and its non-Abelian extension  $SU(2)_Q$ . The discrete symmetries include translations ( $D_i$ ) along the two primitive lattice vectors of the honeycomb lattice, rotations ( $O$ ) by 60 degrees around the center of a hexagon, and reflections ( $R$ ) at the  $x_1$ -axis going through the center of the hexagon. There is also time reversal which is implemented by an anti-unitary operator  $T$ . This symmetry will be considered later on in the effective field theory framework. Furthermore, in the construction of the effective field theory for magnons and holes, it will turn out to be useful to incorporate the combined symmetry  $O'$  consisting of a spatial rotation  $O$  and a global  $SU(2)_s$  spin rotation  $g = i\sigma_2$ . Likewise, we define the composed transformation  $T'$ , consisting of a regular time-reversal  $T$  and the specific spin rotation  $g = i\sigma_2$ .

In [32, 33], Yang and Zhang proved the existence of a non-Abelian extension of the  $U(1)_Q$  fermion number symmetry in the half-filled Hubbard model. This pseudospin symmetry contains  $U(1)_Q$  as a subgroup. The  $SU(2)_Q$  symmetry is realized on the square as well as on the honeycomb lattice and is generated by the three operators

$$Q^+ = \sum_x (-1)^x c_{x\uparrow}^\dagger c_{x\downarrow}^\dagger, \quad Q^- = \sum_x (-1)^x c_{x\downarrow} c_{x\uparrow},$$

$$Q^3 = \sum_x \frac{1}{2} (c_{x\uparrow}^\dagger c_{x\uparrow} + c_{x\downarrow}^\dagger c_{x\downarrow} - 1) = \frac{1}{2} Q. \quad (5)$$

The factor  $(-1)^x$  distinguishes between the two triangular sublattices  $A$  and  $B$  of the honeycomb lattice. Defining  $Q^1$  and  $Q^2$  through  $Q^\pm = Q^1 \pm iQ^2$ , one readily shows that the  $SU(2)_Q$  Lie-algebra  $[Q^a, Q^b] = i\varepsilon_{abc}Q^c$ , with  $a, b, c \in \{1, 2, 3\}$ , indeed is satisfied and that  $[H, \vec{Q}] = 0$  with  $\vec{Q} = (Q^1, Q^2, Q^3)$  for the Hubbard Hamiltonian with  $\mu = 0$ .

In order to write the Hubbard Hamiltonian Eq.(2) or Eq.(4) in a manifestly invariant form under  $SU(2)_s \times SU(2)_Q$ , we arrange the fermion operators in a  $2 \times 2$  matrix-valued operator, arriving at the fermion representation

$$C_x = \begin{pmatrix} c_{x\uparrow} & (-1)^x c_{x\downarrow}^\dagger \\ c_{x\downarrow} & -(-1)^x c_{x\uparrow}^\dagger \end{pmatrix}. \quad (6)$$

This allows us to write down the Hubbard Hamiltonian in the manifestly  $SU(2)_s$ ,  $U(1)_Q$ ,  $D_i$ ,  $O$ ,  $O'$  and  $R$  invariant form

$$H = -\frac{t}{2} \sum_{x,i} \text{Tr}[C_x^\dagger C_{x+i} + C_{x+i}^\dagger C_x] + \frac{U}{12} \sum_x \text{Tr}[C_x^\dagger C_x C_x^\dagger C_x] - \frac{\mu}{2} \sum_x \text{Tr}[C_x^\dagger C_x \sigma_3]. \quad (7)$$

The  $\sigma_3$  Pauli matrix in the chemical potential term prevents the Hubbard Hamiltonian from being invariant under  $SU(2)_Q$  away from half-filling. For  $\mu \neq 0$ ,  $SU(2)_Q$  is explicitly broken down to its subgroup  $U(1)_Q$ . In addition, the pseudospin symmetry is realized in Eq.(7) only for nearest-neighbor hopping. As soon as next-to-nearest-neighbor hopping is included, the  $SU(2)_Q$  invariance gets lost even for  $\mu = 0$ . The continuous  $SU(2)_Q$  symmetry contains a discrete particle-hole symmetry. Although this pseudospin symmetry is not present in real materials, it will play an important role in the construction of the effective field theory. The identification of the final effective fields for holes will lead us to explicitly break the  $SU(2)_Q$  symmetry in subsection 2.3.

## 2.2. Effective field theory for magnons

In this section we review the construction of the effective theory for antiferromagnetic magnons on the honeycomb lattice. The basic object in the effective theory is the staggered magnetization order parameter of the antiferromagnet, which is described by a unit-vector field

$$\vec{e}(x) = (\sin \theta(x) \cos \varphi(x), \sin \theta(x) \sin \varphi(x), \cos \theta(x)), \quad (8)$$

in the coset space  $SU(2)_s/U(1)_s = S^2$ , where  $x = (x_1, x_2, t)$  denotes a point in (2+1)-dimensional space-time. A key ingredient for constructing the effective field theory is the nonlinear realization of the global  $SU(2)_s$  spin symmetry which is spontaneously broken down to its  $U(1)_s$  subgroup, which is discussed in detail in Ref. [19].

It turns out that the above parametrization of the magnon degrees of freedom through the vector  $\vec{e}(x)$  is not appropriate for this construction. Rather, one uses composite magnon fields  $v_\mu(x)$  whose components will be used to couple the magnons to the fermions. The composite magnon field is defined by

$$v_\mu(x) = u(x) \partial_\mu u(x)^\dagger, \quad (9)$$

where the matrix  $u(x)$  is related to the original magnetization vector  $\vec{e}(x) = (e_1(x), e_2(x), e_3(x))$  by

$$\begin{aligned} u(x) &= \frac{1}{\sqrt{2(1+e_3(x))}} \begin{pmatrix} 1 + e_3(x) & e_1(x) - ie_2(x) \\ -e_1(x) - ie_2(x) & 1 + e_3(x) \end{pmatrix} \\ &= \begin{pmatrix} \cos\left(\frac{\theta(x)}{2}\right) & \sin\left(\frac{\theta(x)}{2}\right) \exp(-i\varphi(x)) \\ -\sin\left(\frac{\theta(x)}{2}\right) \exp(i\varphi(x)) & \cos\left(\frac{\theta(x)}{2}\right) \end{pmatrix}. \end{aligned} \quad (10)$$



The coupling of magnons to holes is then realized through the matrix-valued anti-Hermitian field

$$v_\mu(x) = iv_\mu^a(x)\sigma_a, \quad v_\mu^\pm(x) = v_\mu^1(x) \mp iv_\mu^2(x), \quad (11)$$

which decomposes into an Abelian "gauge" field  $v_\mu^3(x)$  and two vector fields  $v_\mu^\pm(x)$  "charged" under the unbroken subgroup  $U(1)_s$ . Here  $\vec{\sigma}$  are the Pauli matrices. These fields have a well-defined transformation behavior under the symmetries which the effective theory inherits from the underlying microscopic  $t$ - $J$  model:

$$\begin{aligned} SU(2)_s : \quad & v_\mu(x)' = h(x)(v_\mu(x) + \partial_\mu)h(x)^\dagger, \\ D_i : \quad & D_i v_\mu(x) = v_\mu(x), \\ O : \quad & O v_1(x) = \tau(Ox) \left\{ \frac{1}{2}v_1(Ox) + \frac{\sqrt{3}}{2}v_2(Ox) + \frac{1}{2}\partial_1 + \frac{\sqrt{3}}{2}\partial_2 \right\} \tau(Ox)^\dagger, \\ & O v_2(x) = \tau(Ox) \left\{ -\frac{\sqrt{3}}{2}v_1(Ox) + \frac{1}{2}v_2(Ox) - \frac{\sqrt{3}}{2}\partial_1 + \frac{1}{2}\partial_2 \right\} \tau(Ox)^\dagger, \\ & O v_t(x) = \tau(Ox)(v_t(Ox) + \partial_t)\tau(Ox)^\dagger, \\ R : \quad & R v_1(x) = v_1(Rx), \quad R v_2(x) = -v_2(Rx), \\ & R v_t(x) = v_t(Rx), \\ T : \quad & T v_i(x) = \tau(Tx)(v_i(Tx) + \partial_i)\tau(Tx)^\dagger, \\ & T v_t(x) = -\tau(Tx)(v_t(Tx) + \partial_t)\tau(Tx)^\dagger. \end{aligned} \quad (12)$$

In the above symmetry transformations, we have introduced the matrix  $\tau(x)$ ,

$$\tau(x) = \begin{pmatrix} 0 & -\exp(-i\varphi(x)) \\ \exp(i\varphi(x)) & 0 \end{pmatrix}. \quad (13)$$

Finally, the Abelian "gauge" transformation

$$h(x) = \exp(i\alpha(x)\sigma_3) \quad (14)$$

belongs to the unbroken  $U(1)_s$  subgroup of  $SU(2)_s$  and acts on the composite vector fields as

$$\begin{aligned} v_\mu^3(x)' &= v_\mu^3(x) - \partial_\mu\alpha(x), \\ v_\mu^\pm(x)' &= v_\mu^\pm(x) \exp(\pm 2i\alpha(x)). \end{aligned} \quad (15)$$

The magnon action, in terms of the composite magnon field  $v_\mu(x)$ , can now be expressed as

$$S[v_\mu^\pm] = \int d^2x dt \, 2\rho_s \left( v_i^+ v_i^- + \frac{1}{c^2} v_t^+ v_t^- \right). \quad (16)$$

Although the expression  $v_\mu^+ v_\mu^-$  looks like a mass term of a charged vector field, it is just the kinetic term of a massless Goldstone boson, since it contains derivatives acting on  $u(x)$ .

### 2.3. Effective field theory for holes and magnons

Analytic calculations as well as Monte Carlo simulations in  $t$ - $J$ -like models on the honeycomb lattice have revealed that at small doping holes occur in pockets centered at lattice momenta  $k^\alpha = -k^\beta = (0, \frac{4\pi}{3\sqrt{3}a})$ , and their copies in the periodic Brillouin zone [34, 35]. The honeycomb lattice, illustrated in figure 1, is a bipartite non-Bravais lattice which consists of two triangular Bravais sublattices. The corresponding Brillouin zone and the location of the corresponding hole pockets are shown in figure 2. The single-hole dispersion relation for the  $t$ - $J$  model on the honeycomb lattice is illustrated in figure 3.

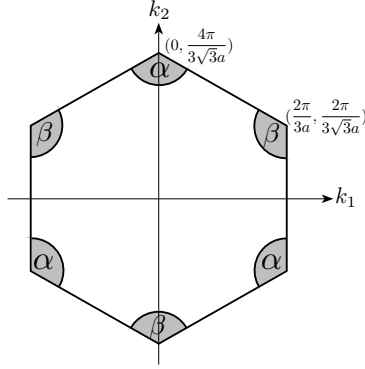


**Figure 2.** Brillouin zone of the honeycomb lattice with corresponding hole pockets.

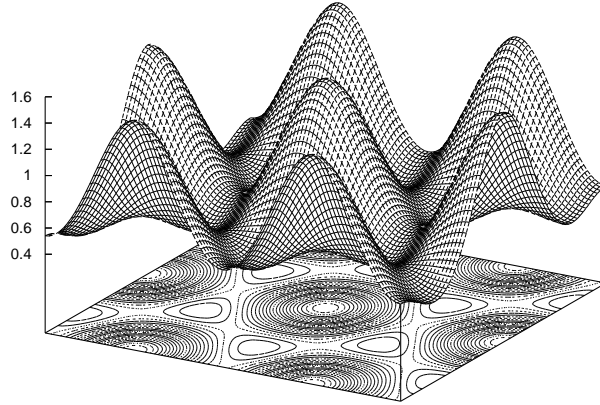


**Figure 3.** Energy-momentum dispersion relation  $E_h(k)/t$  for a single hole in the  $t$ - $J$  model on the honeycomb lattice for  $J/t = 2$ .

The effective field theory is defined in the space-time continuum and the holes are described by Grassmann-valued fields  $\psi_s^f(x)$  carrying a "flavor" index  $f = \alpha, \beta$  that characterizes the corresponding hole pocket. The index  $s = \pm$  denotes spin parallel (+) or antiparallel (−) to the local staggered magnetization. Under the various symmetry operations the hole fields transform as

$$\begin{aligned}
 SU(2)_s : \quad & \psi_\pm^f(x)' = \exp(\pm i\alpha(x))\psi_\pm^f(x), \\
 U(1)_Q : \quad & Q\psi_\pm^f(x) = \exp(i\omega)\psi_\pm^f(x), \\
 D_i : \quad & D_i\psi_\pm^f(x) = \exp(ik_i^f a_i)\psi_\pm^f(x), \\
 O : \quad & O\psi_\pm^\alpha(x) = \mp \exp(\mp i\varphi(Ox) \pm i\frac{2\pi}{3})\psi_\mp^\beta(Ox), \\
 & O\psi_\pm^\beta(x) = \mp \exp(\mp i\varphi(Ox) \mp i\frac{2\pi}{3})\psi_\mp^\alpha(Ox), \\
 R : \quad & R\psi_\pm^\alpha(x) = \psi_\pm^\beta(Rx), \quad R\psi_\pm^\beta(x) = \psi_\pm^\alpha(Rx),
 \end{aligned}$$

$$\begin{aligned}
T: \quad & {}^T\psi_{\pm}^{\alpha}(x) = \exp(\mp i\varphi(Tx))\psi_{\pm}^{\beta\dagger}(Tx), \\
& {}^T\psi_{\pm}^{\beta}(x) = \exp(\mp i\varphi(Tx))\psi_{\pm}^{\alpha\dagger}(Tx), \\
& {}^T\psi_{\pm}^{\alpha\dagger}(x) = -\exp(\pm i\varphi(Tx))\psi_{\pm}^{\beta}(Tx), \\
& {}^T\psi_{\pm}^{\beta\dagger}(x) = -\exp(\pm i\varphi(Tx))\psi_{\pm}^{\alpha}(Tx).
\end{aligned} \tag{17}$$

Here  $U(1)_Q$  is the fermion number symmetry of the holes. Interestingly, in the effective continuum theory the location of holes in lattice momentum space manifests itself as a "charge"  $k_i^f$  under the displacement symmetry  $D_i$ .

Now that the relevant low-energy degrees of freedom have been identified and the transformation rules of the corresponding fields have been worked out, the construction of the effective action is uniquely determined. The low-energy effective action of magnons and holes is constructed as a derivative expansion. At low energies, terms with a small number of derivatives dominate the dynamics. Since the holes are heavy nonrelativistic fermions, one time-derivative counts like two spatial derivatives. Here we limit ourselves to terms with at most one temporal or two spatial derivatives. One then constructs all terms consistent with the symmetries listed above. The effective action can be written as

$$S[\psi_{\pm}^{f\dagger}, \psi_{\pm}^f, v_{\mu}^{\pm}, v_{\mu}^3] = \int d^2x dt \sum_{n_{\psi}} \mathcal{L}_{n_{\psi}}, \tag{18}$$

where  $n_{\psi}$  denotes the number of fermion fields that the various terms contain. The leading terms in the pure magnon sector take the form

$$\mathcal{L}_0 = 2\rho_s \left( v_i^+ v_i^- + \frac{1}{c^2} v_t^+ v_t^- \right). \tag{19}$$

The leading terms with two fermion fields (containing at most one temporal or two spatial derivatives), describing the propagation of holes as well as their couplings to magnons, are given by

$$\begin{aligned}
\mathcal{L}_2 = \sum_{f=\alpha,\beta; s=+,-} \bigg[ & M\psi_s^{f\dagger}\psi_s^f + \psi_s^{f\dagger}D_t\psi_s^f + \frac{1}{2M}D_i\psi_s^{f\dagger}D_i\psi_s^f + \Lambda\psi_s^{f\dagger}(isv_1^s + \sigma_f v_2^s)\psi_{-s}^f \\
& + iK[(D_1 + is\sigma_f D_2)\psi_s^{f\dagger}(v_1^s + is\sigma_f v_2^s)\psi_{-s}^f \\
& - (v_1^s + is\sigma_f v_2^s)\psi_s^{f\dagger}(D_1 + is\sigma_f D_2)\psi_{-s}^f] \\
& + \sigma_f L\psi_s^{f\dagger}\epsilon_{ij}f_{ij}^3\psi_s^f + N_1\psi_s^{f\dagger}v_i^s v_i^{-s}\psi_s^f \\
& + is\sigma_f N_2(\psi_s^{f\dagger}v_1^s v_2^{-s}\psi_s^f - \psi_s^{f\dagger}v_2^s v_1^{-s}\psi_s^f) \bigg].
\end{aligned} \tag{20}$$

Here  $M$  is the rest mass and  $M'$  is the kinetic mass of a hole,  $\Lambda$  and  $K$  are hole-one-magnon couplings, while  $L$ ,  $N_1$ , and  $N_2$  are hole-two-magnon couplings. Note that all low-energy constants are real-valued. The sign  $\sigma_f$  is  $+$  for  $\alpha$  and  $-$  for  $\beta$ . We have introduced the field strength tensor of the composite Abelian "gauge" field

$$f_{ij}^3(x) = \partial_i v_j^3(x) - \partial_j v_i^3(x), \tag{21}$$

and the covariant derivatives  $D_t$  and  $D_i$  acting on  $\psi_{\pm}^f(x)$  as

$$\begin{aligned}
D_t\psi_{\pm}^f(x) &= \left[ \partial_t \pm iv_t^3(x) - \mu \right] \psi_{\pm}^f(x), \\
D_i\psi_{\pm}^f(x) &= \left[ \partial_i \pm iv_i^3(x) \right] \psi_{\pm}^f(x).
\end{aligned} \tag{22}$$

The chemical potential  $\mu$  enters the covariant time-derivative like an imaginary constant vector potential for the fermion number symmetry  $U(1)_Q$ . It is remarkable that the term proportional to  $\Lambda$  with just a single (uncontracted) spatial derivative satisfies all symmetries. Due to the small number of derivatives it contains, this term dominates the low-energy dynamics of a lightly hole-doped antiferromagnet on the honeycomb lattice. Interestingly, for antiferromagnets on the square lattice, a corresponding term, which was first identified by Shraiman and Siggia, is also present in the hole-doped case [20]. On the other hand, a similar term is forbidden by symmetry reasons in the electron-doped case [21]. For the honeycomb geometry we even identify a second hole-one-magnon coupling,  $K$ , whose contribution, however, is sub-leading. Interestingly, hole- or electron-doped antiferromagnets on the square lattice do not allow terms containing the field-strength tensor  $f_{ij}$  in  $\mathcal{L}_2$ .

Finally, the leading terms without derivatives and with four fermion fields are given by

$$\begin{aligned} \mathcal{L}_4 = & \sum_{s=+,-} \left\{ \frac{G_1}{2} (\psi_s^{\alpha\dagger} \psi_s^\alpha \psi_{-s}^{\alpha\dagger} \psi_{-s}^\alpha + \psi_s^{\beta\dagger} \psi_s^\beta \psi_{-s}^{\beta\dagger} \psi_{-s}^\beta) \right. \\ & \left. + G_2 \psi_s^{\alpha\dagger} \psi_s^\alpha \psi_s^{\beta\dagger} \psi_s^\beta + G_3 \psi_s^{\alpha\dagger} \psi_s^\alpha \psi_{-s}^{\beta\dagger} \psi_{-s}^\beta \right\}. \end{aligned} \quad (23)$$

The low-energy four-fermion coupling constants  $G_1$ ,  $G_2$ , and  $G_3$  are also real-valued. Although potentially invariant under all symmetries, terms with two identical hole fields vanish due to the Pauli principle.

It is important to note that in the above construction of the effective Lagrangian for the  $t$ - $J$  model which contains holes only, a crucial step was to identify the degrees of freedom that correspond to the holes. In order to remove the electron degrees of freedom one has to explicitly break the particle-hole  $SU(2)_Q$  symmetry, leaving the ordinary fermion number symmetry  $U(1)_Q$  intact. This task can be achieved by constructing all possible fermionic mass terms that are invariant under the various symmetries. Picking the eigenvectors which correspond to the lowest eigenvalues of the mass matrices then allows one to separate electrons from holes. This procedure is described in detail in Ref. [22]

We would like to point out that the leading order terms in the effective Lagrangian for magnons and holes constructed above exhibit two accidental global symmetries. First, we notice that for  $c \rightarrow \infty$  and without the term proportional to  $iK$  in  $\mathcal{L}_2$ , Eqs.(19) and (20), have an accidental Galilean boost symmetry. Although the Galilean boost symmetry is explicitly broken at higher orders of the derivative expansion, this symmetry has physical implications: The leading one-magnon exchange between two holes, to be discussed in the next section, can be investigated in their rest frame without loss of generality.

In addition, we notice an accidental global rotation symmetry  $O(\gamma)$ . Except for the term proportional to  $iK$ ,  $\mathcal{L}_2$  of Eq.(20) is invariant under a continuous spatial rotation by an angle  $\gamma$ . This symmetry is not present in the  $\Lambda$ -term of the square lattice. The  $O(\gamma)$  invariance has some interesting implications for the spiral phases in a lightly doped antiferromagnet on the honeycomb lattice, as we will see in the next section.

### 3. Applications

In this section we will consider two nontrivial applications of the effective Lagrangian constructed above: The emergence of spiral phases in the staggered magnetization vector order parameter and the formation of two-hole bound states.

#### 3.1. Spiral phases

Let us first investigate whether so-called spiral phases in the staggered magnetization can occur upon hole-doping. This problem has been studied before using microscopic theories

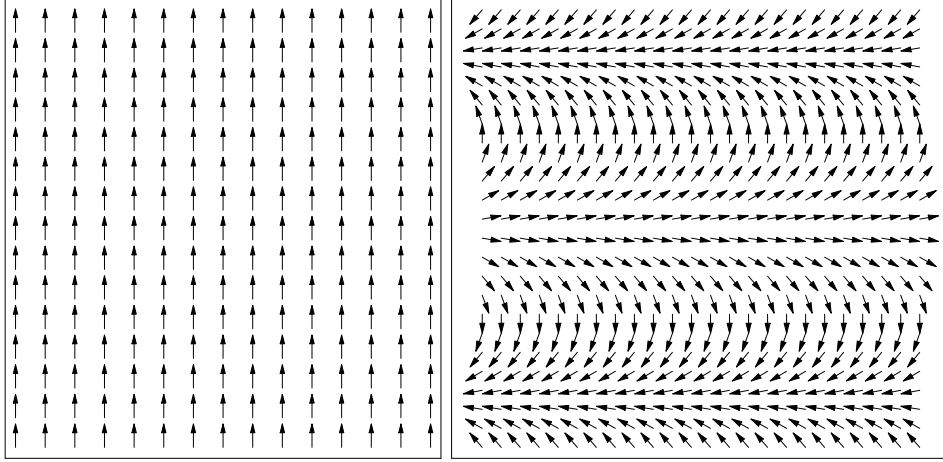


**Figure 4.** Left panel: Homogeneous phase with constant staggered magnetization. Right panel: Spiral phase with helical structure in the staggered magnetization.

[36, 37, 38, 39]. In Ref. [24] the problem was studied systematically in the case of a square lattice using effective Lagrangians. Here we consider the honeycomb lattice – details of the calculation can be found in Ref. [25].

In our study we assume that the holes are doped into the system homogeneously and thus limit ourselves to configurations of the staggered magnetization that are either homogeneous themselves or generate a constant background field  $v_i(x)$  for the charge carriers. As was shown in [24], the most general configuration of this kind represents a spiral in the staggered magnetization. We also assume that four-fermion contact interactions are weak and take them into account perturbatively – again, for details see Refs.[21, 24].

When one populates the various hole pockets, one must distinguish a total of four different cases. First we have  $\alpha$ -pockets and  $\beta$ -pockets. Moreover, the energy eigenstates of a hole pocket  $f$  can acquire two values,  $E_-^f$  and  $E_+^f$ , where the former corresponds to the lower energy. One thus starts considering the case of populating all four hole pockets, i.e. with both flavors  $f = \alpha, \beta$  and with both energy indices  $\pm$ . One then proceeds with populating only three, only two and, finally, only one hole pocket. This gives rise to various phases of the staggered magnetization, which can be either homogeneous or a spiral phase as depicted in figure 4.

More precisely, the energy densities of the various phases take the form

$$\epsilon_i = \epsilon_0 + Mn + \frac{1}{2}\kappa_i n^2. \quad (24)$$

Here  $\epsilon_0$  is the energy density of the system at half-filling and  $n$  is the total density of holes. The index  $i$  refers to the number of hole pockets that are populated in the corresponding phase. The compressibilities  $\kappa_i$  are given by

$$\begin{aligned} \kappa_1 &= \frac{2\pi}{M'} - \frac{\Lambda^2}{4\rho_s}, \\ \kappa_2 &= \frac{\pi}{M'} - \frac{\Lambda^2}{4\rho_s} + \frac{1}{4}(G_2 + G_3), \\ \kappa_3 &= \frac{2\pi}{3M'} \left( 1 - \frac{1}{8} \frac{M'\Lambda^2}{3\pi\rho_s - M'\Lambda^2} \right) \end{aligned}$$

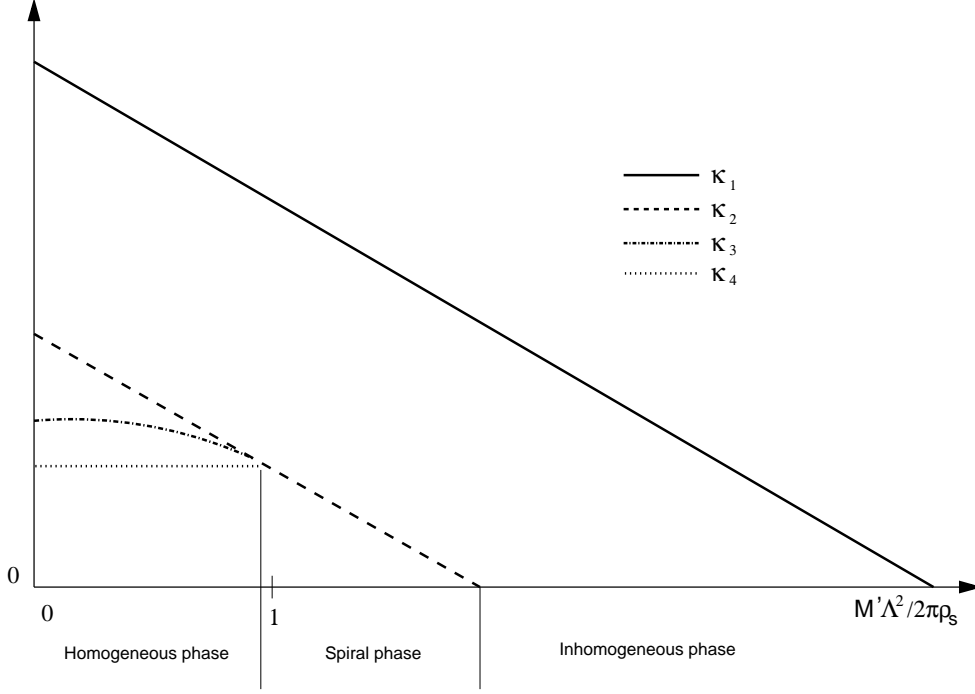


**Figure 5.** The compressibilities  $\kappa_i$  as functions of  $M'\Lambda^2/2\pi\rho_s$  determine the stability ranges of the various phases. A homogeneous phase, a spiral, or an inhomogeneous phase are energetically favorable, for large, intermediate, and small values of  $\rho_s$ , respectively.

$$\begin{aligned}
& + \frac{4\pi\rho_s - M'\Lambda^2}{(3\pi\rho_s - M'\Lambda^2)^2} \frac{1}{16} \left[ 8(G_1 + G_2 + G_3)\pi\rho_s \right. \\
& \left. - (4G_1 + 3G_2 + 3G_3)M'\Lambda^2 \right], \\
\kappa_4 &= \frac{\pi}{2M'} + \frac{1}{4}(G_1 + G_2 + G_3),
\end{aligned} \tag{25}$$

and shown in figure 5 as functions of  $M'\Lambda^2/2\pi\rho_s$ . For large values of  $\rho_s$ , spiral phases cost a large amount of magnetic energy and the homogeneous phase is more stable. To be more precise, in this regime one has  $\kappa_4 < \kappa_3 < \kappa_2 < \kappa_1$ . Notice that  $\kappa_1$  is always larger than  $\kappa_2$  for any value of  $\rho_s$ . As  $\rho_s$  decreases and reaches the value

$$\rho_s = \frac{M'\Lambda^2}{2\pi} + \frac{(M')^2\Lambda^2 G_1}{4\pi^2}, \tag{26}$$

at leading order in the 4-fermi couplings one finds  $\kappa_2 = \kappa_3 = \kappa_4$ . For smaller values of  $\rho_s$ , the two-pocket spiral is energetically favored until  $\kappa_2$  becomes negative and the system becomes unstable against the formation of spatial inhomogeneities of a yet undetermined type.

Interestingly, unlike in the square lattice case, due to the accidental continuous  $O(\gamma)$  spatial rotation symmetry, at leading order a spiral does not have an a priori preferred spatial direction. It is instructive to compare the results presented here with the results obtained in the square lattice case [24]. Qualitatively the stability ranges of various phases are the same for both lattice geometries except that the one-pocket spiral is never energetically favored on the honeycomb lattice while it is favorable in a small parameter regime on the square lattice.

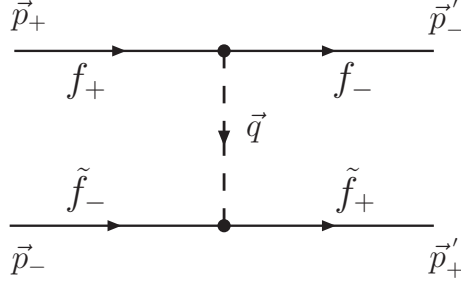


**Figure 6.** Tree-level Feynman diagram for one-magnon exchange between two holes.

### 3.2. Two-hole bound states

In the effective theory framework, at low energies, holes interact with each other via magnon exchange. Since the long-range dynamics is dominated by one-magnon exchange, we will calculate the one-magnon exchange potentials between two holes of the same flavor  $\alpha$  and  $\beta$  and of different flavor, and then address the question regarding the formation of two-hole bound states. The same problem was also considered in Refs. [40, 41, 42] using microscopic theories.

We expand in the magnon fluctuations  $m_1(x)$  and  $m_2(x)$  around the ordered staggered magnetization

$$\vec{e}(x) = \left( \frac{m_1(x)}{\sqrt{\rho_s}}, \frac{m_2(x)}{\sqrt{\rho_s}}, 1 \right) + \mathcal{O}(m^2). \quad (27)$$

For the composite magnon fields this implies

$$\begin{aligned} v_\mu^\pm(x) &= \frac{1}{2\sqrt{\rho_s}} \partial_\mu [m_2(x) \pm i m_1(x)] + \mathcal{O}(m^3), \\ v_\mu^3(x) &= \frac{1}{4\rho_s} [m_1(x) \partial_\mu m_2(x) - m_2(x) \partial_\mu m_1(x)] + \mathcal{O}(m^4). \end{aligned} \quad (28)$$

Vertices with  $v_\mu^3(x)$  involve at least two magnons, such that one-magnon exchange results from vertices with  $v_\mu^\pm(x)$  only. As a consequence, two holes can exchange a single magnon only if they have anti-parallel spins (+ and -), which are both flipped in the magnon-exchange process. We denote the momenta of the incoming and outgoing holes by  $\vec{p}_\pm$  and  $\vec{p}'_\pm$ , respectively. The momentum carried by the exchanged magnon is denoted by  $\vec{q}$ . The incoming and outgoing holes are asymptotic free particles with momentum  $\vec{p} = (p_1, p_2)$  and energy  $E(\vec{p}) = M + p_i^2/2M'$ . One-magnon exchange between two holes is associated with the Feynman diagram in figure 6. Evaluating these Feynman diagrams, one finds the resulting potentials for the various combinations of flavors  $f, \tilde{f} \in \{\alpha, \beta\}$  and couplings  $F, \tilde{F} \in \{\Lambda, K\}$ .

The leading contribution to the low-energy physics, as we noted earlier, comes from the  $\Lambda$  vertex. From here on, we therefore concentrate on the potential with two  $\Lambda$  vertices only. In coordinate space the  $\Lambda\Lambda$ -potentials are given by

$$\langle \vec{r}'_+ \vec{r}'_- | V_{\Lambda\Lambda}^{f\tilde{f}} | \vec{r}_+ \vec{r}_- \rangle = V_{\Lambda\Lambda}^{f\tilde{f}}(\vec{r}) \delta(\vec{r}_+ - \vec{r}'_-) \delta(\vec{r}_- - \vec{r}'_+), \quad (29)$$

with

$$V_{\Lambda\Lambda}^{ff}(\vec{r}) = -\frac{\Lambda^2}{2\rho_s} \delta^{(2)}(\vec{r}), \quad V_{\Lambda\Lambda}^{ff'}(\vec{r}) = \frac{\Lambda^2}{2\pi\rho_s \vec{r}^2} \exp(2i\sigma_f \varphi). \quad (30)$$

Here  $\vec{r} = \vec{r}_+ - \vec{r}_-$  denotes the distance vector between the two holes and  $\varphi$  is the angle between  $\vec{r}$  and the  $x_1$ -axis. The  $\delta$ -functions in Eq.(29) ensure that the holes do not change their position

during the magnon exchange. Note that the one-magnon exchange potentials are instantaneous although magnons travel with the finite speed  $c$ . Retardation effects occur only at higher orders.

Interestingly, in the  $\Lambda\Lambda$  channel, one-magnon exchange over long distances between two holes can only happen for holes of opposite flavor. For two holes of the same flavor, one-magnon exchange acts as a contact interaction. Here we concentrate on the long-range physics of weakly bound states of holes and therefore will only consider the binding of holes of different flavor.

Let us therefore investigate the Schrödinger equation for the relative motion of two holes with flavors  $\alpha$  and  $\beta$ . In the following, we will take care of short distance interactions by imposing a hard-core boundary condition on the pair's wave function. Due to the accidental Galilean boost invariance, without loss of generality, we can consider the hole pair in its rest frame. The total kinetic energy of the two holes is given by

$$T = \sum_{f=\alpha,\beta} T^f = \sum_{f=\alpha,\beta} \frac{p_i^2}{2M'} = \frac{p_i^2}{M'}. \quad (31)$$

We now introduce the two probability amplitudes  $\Psi_1(\vec{r})$  and  $\Psi_2(\vec{r})$  which represent the two flavor-spin combinations  $\alpha_+\beta_-$  and  $\alpha_-\beta_+$ , respectively, with the distance vector  $\vec{r}$  to point from the  $\beta$  to the  $\alpha$  hole. Because the holes undergo a spin flip during the magnon exchange, the two probability amplitudes are coupled through the magnon exchange potentials and the Schrödinger equation describing the relative motion of the hole pair is a two-component equation. Using the explicit form of the potentials, it takes the form

$$\begin{pmatrix} -\frac{1}{M'}\Delta & \gamma\frac{1}{r^2}\exp(-2i\varphi) \\ \gamma\frac{1}{r^2}\exp(2i\varphi) & -\frac{1}{M'}\Delta \end{pmatrix} \begin{pmatrix} \Psi_1(\vec{r}) \\ \Psi_2(\vec{r}) \end{pmatrix} = E \begin{pmatrix} \Psi_1(\vec{r}) \\ \Psi_2(\vec{r}) \end{pmatrix}, \quad (32)$$

with

$$\gamma = \frac{\Lambda^2}{2\pi\rho_s}. \quad (33)$$

As it turns out, magnon-mediated forces can lead to bound states only if the low-energy constant  $\Lambda$  is larger than a critical value given by

$$\Lambda_c = \sqrt{\frac{2\pi\rho_s}{M'}}. \quad (34)$$

Interestingly, the same critical value also arose in the investigation of spiral phases in a lightly doped antiferromagnet on the honeycomb lattice in Eq.(26). There it marked the point where spiral phases become energetically favorable compared to the homogeneous phase.

With the separation ansatz

$$\Psi_1(r, \varphi) = R_1(r) \exp(im_1\varphi), \quad \Psi_2(r, \varphi) = R_2(r) \exp(im_2\varphi), \quad (35)$$

the relevant equation which is associated with an attractive potential and thus potentially leads to the formation of bound states amounts to

$$\left[ -\left( \frac{d^2}{dr^2} + \frac{1}{r} \frac{d}{dr} \right) + (1 - \gamma M') \frac{1}{r^2} \right] R(r) = -M'|E|R(r), \quad (36)$$

with  $E = -|E|$  and  $R(r) = R_1(r) - R_2(r)$ . It has to be pointed out that this equation refers to the case  $m_1 = -1$  and  $m_2 = 1$  where the system (32) can be decoupled (see [22]).

The same equation also occurred in the square lattice case [20, 23] and can be solved along the same lines. As it stands, the equation is ill-defined because the  $1/r^2$  potential is too singular



at the origin. However, we have not yet included the contact interaction proportional to the 4-fermion coupling  $G_3$ . Here, in order to keep the calculation analytically feasible, we model the short-range repulsion by a hard core radius  $r_0$ , i.e. we require  $R(r_0) = 0$  for  $r \leq r_0$ . Eq.(36) is solved by a modified Bessel function

$$R(r) = AK_\nu(\sqrt{M'|E|r}), \quad \nu = i\sqrt{\gamma M' - 1}, \quad (37)$$

with  $A$  being a normalization constant. Demanding that the wave function vanishes at the hard core radius gives a quantization condition for the bound state energy. The quantum number  $n$  then labels the  $n$ -th excited state. For large  $n$ , the binding energy is given by

$$E_n \sim -\frac{1}{M'r_0^2} \exp\left(\frac{-2\pi n}{\sqrt{\gamma M' - 1}}\right). \quad (38)$$

The binding is exponentially small in  $n$  and there are infinitely many bound states. While the highly excited states have exponentially small energy, for sufficiently small  $r_0$  the ground state could have a small size and be strongly bound. However, for short-distance physics the effective theory should not be trusted quantitatively. Still, as long as the binding energy is small compared to the relevant high-energy scales, our result is valid and receives only small corrections from higher-order effects such as two-magnon exchange.

We now turn to the discussion of the angular part of the wave equation. The ansatz (35) leads to the following solution for the ground state wave function

$$\Psi(r, \varphi) = \begin{pmatrix} \Psi_1(\vec{r}) \\ \Psi_2(\vec{r}) \end{pmatrix} = R(r) \begin{pmatrix} \exp(-i\varphi) \\ -\exp(i\varphi) \end{pmatrix}. \quad (39)$$

Under the 60 degrees rotation  $O$ , using the transformation rules of Eq.(17), one obtains

$$O\Psi(r, \varphi) = -\Psi(r, \varphi). \quad (40)$$

Interestingly, the wave function for the ground state of two holes of flavors  $\alpha$  and  $\beta$  thus exhibits  $f$ -wave symmetry.<sup>1</sup> The corresponding probability distribution depicted in figure 7, on the other hand, seems to show  $s$ -wave symmetry. However, the relevant phase information is not visible in this picture, because only the probability density is shown. Interestingly, for two-hole bound states on the square lattice, the wave function for the the ground state of two holes of flavors  $\alpha$  and  $\beta$  shows  $p$ -wave symmetry, while the corresponding probability distribution (which again does not contain the relevant phase information) resembles  $d_{x^2-y^2}$  symmetry [20]. Remarkably, the ground state wave function (39) of a bound hole pair on the honeycomb lattice remains invariant under the reflection symmetry  $R$ , the shift symmetries  $D_i$ , as well as under the accidental continuous rotation symmetry  $O(\gamma)$ .

We find it quite remarkable that the  $f$ -wave character of the two-hole bound state on the honeycomb lattice is an immediate consequence of our systematic effective field theory analysis. The question regarding the true symmetry of the pairing state realized in the dehydrated version of  $\text{Na}_2\text{CoO}_2 \times y \text{H}_2\text{O}$ , still seems to be controversial [43]. Still, a careful analysis of the available experimental data for this compound suggests that the pairing symmetry indeed is  $f$ -wave [44].

#### 4. Conclusions

The effective theory for the insulating antiferromagnetic precursors of high-temperature superconductors is the condensed matter analog of baryon chiral perturbation theory: Magnons

<sup>1</sup> Strictly speaking, the continuum classification scheme of angular momentum eigenstates does not apply here, since we are not dealing with a continuous rotation symmetry.

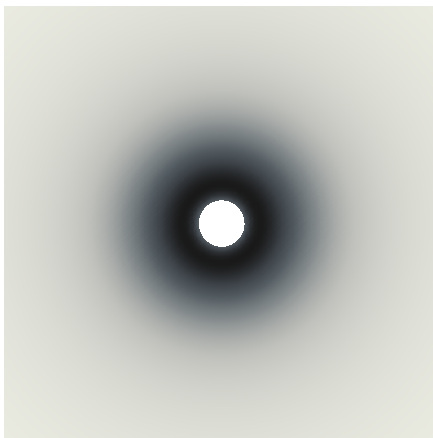


**Figure 7.** *Probability distribution for the ground state of two holes of flavors  $\alpha$  and  $\beta$ .*

play the role of the pseudoscalar mesons, while the holes and electrons are the analog of the baryon octet. We have analyzed the symmetries of the underlying Hubbard and  $t-J$ -type models in detail and reviewed the systematic construction of the effective low-energy field theory for weakly hole-doped antiferromagnets on the honeycomb lattice. The procedure is fully systematic order by order in a derivative expansion of the magnon and hole fields. As two nontrivial applications we have considered the existence of spiral phases in the staggered magnetization order parameter and the formation of two-hole bound states mediated by magnon exchange.

Regarding spiral phases, we have limited ourselves to constant composite vector fields  $v_i(x)$  which implies that the fermions experience a constant background field. Unlike in the square lattice case, due to the accidental continuous  $O(\gamma)$  spatial rotation symmetry, at leading order a spiral does not have an a priori preferred spatial direction. However, since the  $O(\gamma)$  symmetry is broken explicitly by the higher-order terms, once such terms are included, one expects the spiral to align with a lattice direction. We also investigated the stability of spiral phases in the presence of 4-fermion couplings. If these couplings can be treated perturbatively, for sufficiently large values of  $\rho_s$ , the homogeneous phase is energetically favored. With decreasing  $\rho_s$ , a two-pocket spiral becomes energetically more favorable. In contrast to the square lattice case, the one-pocket spiral is never favored. For small values of  $\rho_s$  the two-pocket spiral becomes unstable against the formation of inhomogeneities of a yet undetermined type.

Regarding the formation of two-hole bound states mediated by magnon-exchange, we have studied the effect of the magnon-hole vertex. Again in contrast to the square lattice case, it turned out that the magnon-hole coupling constant  $\Lambda$  must exceed a critical value in order to obtain two-hole bound states. Our analysis implies that the wave function for the ground state of two holes of flavors  $\alpha$  and  $\beta$  exhibits  $f$ -wave symmetry (while the corresponding probability distribution seems to suggest  $s$ -wave symmetry). This is quite different from the square lattice case, where the wave function for the ground state of two holes of flavors  $\alpha$  and  $\beta$  exhibits  $p$ -wave symmetry (while the corresponding probability distribution resembles  $d_{x^2-y^2}$  symmetry).

It is quite remarkable that all these results unambiguously follow from the very few basic assumptions of the systematic low-energy effective theory, such as symmetry, locality, and unitarity. The effective theory provides a theoretical framework in which the low-energy dynamics of lightly hole-doped antiferromagnets can be investigated in a systematic manner. In particular, after the low-energy parameters have been adjusted appropriately, the resulting low-energy physics is completely equivalent to the one of the Hubbard or  $t-J$  model.

## Acknowledgments

C.P.H. would like to thank the members of the Institute for Theoretical Physics at Bern University for their warm hospitality during a visit at which this project was completed. Support by CONACYT grant No. 50744-F is gratefully acknowledged.

## References

- [1] Bednorz J C and Müller K A 1986 *Z. Phys.* B **64** 189
- [2] Weinberg S 1979 *Physica* **96 A** 327
- [3] Gasser J and Leutwyler H 1985 *Nucl. Phys.* B **250** 465
- [4] Gasser J, Sainio M E and Švarc A 1988 *Nucl. Phys.* B **307** 779
- [5] Jenkins E and Manohar A 1991 *Phys. Lett.* B **255** 558
- [6] Bernard V , Kaiser N, Kambor J, and Meissner U-G 1992 *Nucl. Phys.* B **388** 315
- [7] Becher T and Leutwyler H 1999 *Eur. Phys. J. C* **9** 643
- [8] Hasenfratz P and Niedermayer F 1993 *Z. Phys.* B **92** 91
- [9] Leutwyler H 1994 *Phys. Rev.* D **49** 3033
- [10] Leutwyler H 1997 *Helv. Phys. Acta* **70** 275
- [11] Román J M and Soto J 1999 *Int. J. Mod. Phys.* B **13** 755
- [12] Hofmann C P 1999 *Phys. Rev.* B **60** 388
- [13] Hofmann C P 1999 *Phys. Rev.* B **60** 406
- [14] Román J M and Soto J 1999 *Ann. Phys.* **273** 37
- [15] Román J M and Soto J 2000 *Phys. Rev.* B **62** 3300
- [16] Hofmann C P 2002 *Phys. Rev.* B **65** 094430
- [17] Hofmann C P 2010 *Phys. Rev.* B **81** 014416
- [18] Hofmann C P 2011 *Phys. Rev.* B **84** 064414
- [19] Kämpfer F, Moser M and Wiese U-J 2005 *Nucl. Phys.* B **729** 317
- [20] Brügger C, Kämpfer F, Moser M, Pepe M and Wiese U-J 2006 *Phys. Rev.* B **74** 224432
- [21] Brügger C, Hofmann C P, Kämpfer F, Moser M, Pepe M and Wiese U-J 2007 *Phys. Rev.* B **75** 214405
- [22] Kämpfer F, Bessire, B, Wirz, M, Hofmann C P, Jiang F-J and Wiese 2012 to appear in *Phys. Rev.* B
- [23] Brügger C, Kämpfer F, Pepe M and Wiese U-J 2006 *Eur. Phys. J. B* **53** 433
- [24] Brügger C, Hofmann C P, Kämpfer F, Pepe M and Wiese U-J 2007 *Phys. Rev.* B **75** 014421
- [25] Jiang F-J, Kämpfer F, Hofmann C P, and Wiese U-J 2009 *Eur. Phys. J. B* **69** 473
- [26] Gerber U, Hofmann C P, Kämpfer F and Wiese U-J 2010 *Phys. Rev.* B **81** 064414
- [27] Wiese U-J and Ying H P 1994 *Z. Phys.* B **93** 147
- [28] Gerber U, Hofmann C P, Jiang F-J, Nyfeler M and Wiese U-J 2009 *J. Stat. Mech.: Theory Exp.* P03021
- [29] Jiang F-J and Wiese U-J 2011 *Phys. Rev.* B **83** 155120
- [30] Gerber U, Hofmann C P, Jiang F-J, Palma G, Stebler P and Wiese U-J 2011 *J. Stat. Mech.: Theory Exp.* P06002
- [31] Anderson P W 1987 *Science* **235** 1196
- [32] Zhang S 1990 *Phys. Rev. Lett.* **65** 120
- [33] Yang C N and Zhang S C 1990 *Mod. Phys. Lett.* B **4** 759
- [34] Lüscher A , Läuchli A, Zheng W, and Sushkov O 2006 *Phys. Rev.* B **73** 155118
- [35] Jiang F-J, Kämpfer F, Nyfeler M and Wiese U-J 2008 *Phys. Rev.* B **78** 214406
- [36] Shraiman B I and Siggia E D 1988 *Phys. Rev. Lett.* **60** 740; **61** 467; **62** 1564
- [37] Shraiman B I and Siggia E D 1992 *Phys. Rev.* B **46** 8305
- [38] Sushkov O P and Kotov V N 2004 *Phys. Rev.* B **70** 024503
- [39] Kotov V N and Sushkov O P 2004 *Phys. Rev.* B **70** 195105
- [40] Sushkov O P and Flambaum V V 1993 *Physica C* **206** 269
- [41] Kuchiev M J and Sushkov O P 1993 *Physica C* **218** 197
- [42] Flambaum V V, Kuchiev M Y and Sushkov O P 1994 *Physica C* **227** 267
- [43] Ivanova N B, Ovchinnikov S G, Korshunov M M, Eremin I M and Kazak N V 2009 *Phys. Usp.* **52** 789
- [44] Mazin I I and Johannes M D 2005 *Nature Physics* **1** 91